THE ASTROPHYSICAL JOURNAL, 513:294–304, 1999 March 1

THE INTERSTELLAR 4.62 MICRON BAND

Y. J. PENDLETON,[1] A. G. G. M. TIELENS,[2,3] A. T. TOKUNAGA,[3,4] AND M. P. BERNSTEIN[5]

Received 1997 December 22; accepted 1998 October 8

ABSTRACT

We present new 4.5–5.1 μm (2210–1970 cm^{-1}) spectra of embedded protostars, W33 A, AFGL 961 E, AFGL 2136, NGC 7538 IRS 9, and Mon R2 IRS 2, which contain a broad absorption feature located near 4.62 μm (2165 cm^{-1}), commonly referred to in the literature as the "X−C≡N" band. The observed peak positions and widths of the interstellar band agree to within 2.5 cm^{-1} and 5 cm^{-1}, respectively. The strengths of the interstellar 4.62 μm band and the ice absorption features in these spectra are not correlated, which suggests a diversity of environmental conditions for the ices we are observing. We explore several possible carriers of the interstellar band and review possible production pathways through far-ultraviolet photolysis (FUV), ion bombardment of interstellar ice analog mixtures, and acid-base reactions. Good fits to the interstellar spectra are obtained with an organic residue produced through ion bombardment of nitrogen-containing ices or with the OCN^- ion produced either through acid-base reactions or FUV photolysis of NH_3-containing ices.

Subject headings: infrared: ISM: lines and bands — ISM: clouds — ISM: molecules — line: identification — stars: pre–main-sequence

1. INTRODUCTION

More than two decades of infrared astronomical spectroscopy have revealed the importance of dust in the interstellar medium (ISM). Stars and planetary systems form out of dust in dense molecular clouds, the same dust that plays a pivotal role in the heating and cooling of the interstellar gas. Until relatively recently, crucial portions of the infrared spectrum were unavailable to astronomical spectroscopists owing to atmospheric limitations that hinder ground-based efforts, so despite the accumulating body of knowledge, gaps in the spectral observations have remained. The 2–30 μm wavelength region is critically important for the study of organic solids and ices, and with results from the Kuiper Airborne Observatory (KAO) and the *Infrared Space Observatory* (*ISO*), the major gaps in the observational picture are now being filled in. The combination of moderate-resolution spectroscopy in those regions accessible from the ground with the space and airborne observations is providing a more complete inventory of the dust constituents, as well as information regarding the physical locations of dust repositories. Ultimately, the goal is to understand the physical conditions under which interstellar dust features form and evolve.

Here we present moderate-resolution ($R \approx 1200$) infrared spectroscopy in a spectral region that is accessible from the ground. The feature discussed here, the interstellar 4.62 μm (2165 cm^{-1}) band, likely arises from a carbon-nitrogen carrier and may be our most useful diagnostic of processed interstellar ices. The exact identification remains unclear, however, as there are multiple pathways to the production of the band in the laboratory, and different nitrogen-containing precursor molecules have been used. Identifying the production mechanism responsible for the interstellar 4.62 μm band and/or constraining the nitrogen reservoir available for processing will help our understanding of solid-state organic species in space.

The observation and reduction procedures used to obtain the astronomical spectra are discussed in § 2, and the results are presented in § 3. A discussion of possible identifications and formation mechanisms of the interstellar 4.62 μm band are presented in § 4. A summary is given in § 5. The observational details are listed in Table 1, and a compilation of dust optical depth features is presented in Table 2. Optical depth ratios of diagnostic absorption features are provided in Table 3. Summary tables of the candidate species and production pathways are given in Tables 4 and 5, respectively.

2. OBSERVATIONS AND DATA REDUCTION

All the observations presented here were made during 1986 November 17–21 and 1988 July 21–22 at the NASA Infrared Telescope Facility (IRTF) on Mauna Kea using the Cooled Grating Array Spectrometer (CGAS). The CGAS employed a linear 32 element InSb detector (Tokunaga, Smith, & Irvin 1987). Output from detectors 1, 2, 13, and 32 was not used, as these detectors were not operating reliably during the observation run. The observations were made using an aperture of 2.″7 and a north-south chop of 15′. Typical exposure times were 30–60 minutes per source per night. The spectrometer was used in first order with grating B, which provided a resolving power of 1200 (i.e., a spectral resolution element of 0.004 μm [$\approx$1.8 cm^{-1}]). Objects were observed at two grating settings separated by half a resolution element, except for NGC 7538 IRS 9, which was observed once (1989 July) with 0.25 resolution element sampling. For calibration and atmospheric correction purposes, each individual grating setting on an object was either preceded or followed by a standard star located in the same part of the sky that also had a closely matching air mass to that of the source. This process minimized the residual telluric absorption features

[1] NASA Ames Research Center, Mail Stop 245-3, Moffett Field, CA 94035.
[2] Kapteyn Astronomical Institute, P.O. Box 800, 9700 AV, Groningen, NL.
[3] Visiting Astronomer, Infrared Telescope Facility, which is operated by the University of Hawaii under contract with the National Space and Aeronautics Administration.
[4] Institute for Astronomy, University of Hawaii, 2680 Woodlawn Drive, Honolulu, HI 96822.
[5] NASA Ames Research Center, Mail Stop 245-6, Moffett Field, CA 94035, and SETI Institute, Mountain View, CA 94043.

TABLE 1

SUMMARY OF OBSERVATIONS

Source	R.A. (1950)	Decl. (1950)	Date (UT)	Standard
AFGL 2136.....	18 24 14	−25 06 12	1988 Jul 22	BS 7020
AFGL 961 E	6 31 59.1	4 15 10	1986 Nov 17–19	BS 1903
Mon R2 IRS 2	06 05 19.4	−06 22 24	1986 Nov 17–19	BS 1903
W33 A.....	18 11 43.7	−17 53 02	1988 Jul 21	BS 6561
NGC 7538 IRS 9.....	23 11 52.8	61 10 58	1986 Nov 17–19 and 1989 July 20	BS 8571

NOTE.—Units of right ascension are hours, minutes, and seconds, and units of declination are degrees, arcminutes, and arcseconds.

in the reduced spectra. After ratioed spectra were calculated at individual grating settings, the flux levels were adjusted to each other in the overlap region. Mismatches in flux levels, caused by seeing and guiding errors, were typically less than 10%.

The wavelength calibration is discussed in detail in Tielens et al. (1991). The central wavelength of each detector is known to much better precision than the spectral resolution element. Absolute wavelength calibration was provided by an argon discharge lamp attached to the CGAS. Measurements at the telescope show that wavelengths are accurate to about 5×10^{-4} μm (0.23 cm^{-1}), and therefore the shape of an absorption feature is determined to this accuracy. We note that two features separated by less than the Nyquist frequency ($\approx$0.9 cm^{-1}) will not be resolved. All wavelengths are given here in vacuo. Doppler shifts due to the motion of the object are typically very small, and no correction has been applied to the reported spectra.

3. RESULTS

3.1. *The Objects and Their Spectra*

We present new observations of AFGL 2136, AFGL 961 E, Mon R2 IRS 2, W33 A, and NGC 7538 IRS 9. Table 1 contains a list of the objects and their coordinates. These sources are luminous, deeply embedded protostars seen through dense molecular cloud material. The objects in the present paper were chosen to sample the environments of different molecular cloud cores where other absorption features had previously been detected (specifically, H_2O, CO, and silicate). The 4.5–5.1 μm (2222–1960 cm^{-1}) spectrum of W33 A is shown in Figure 1. The 4.5–4.8 μm (2222–2083

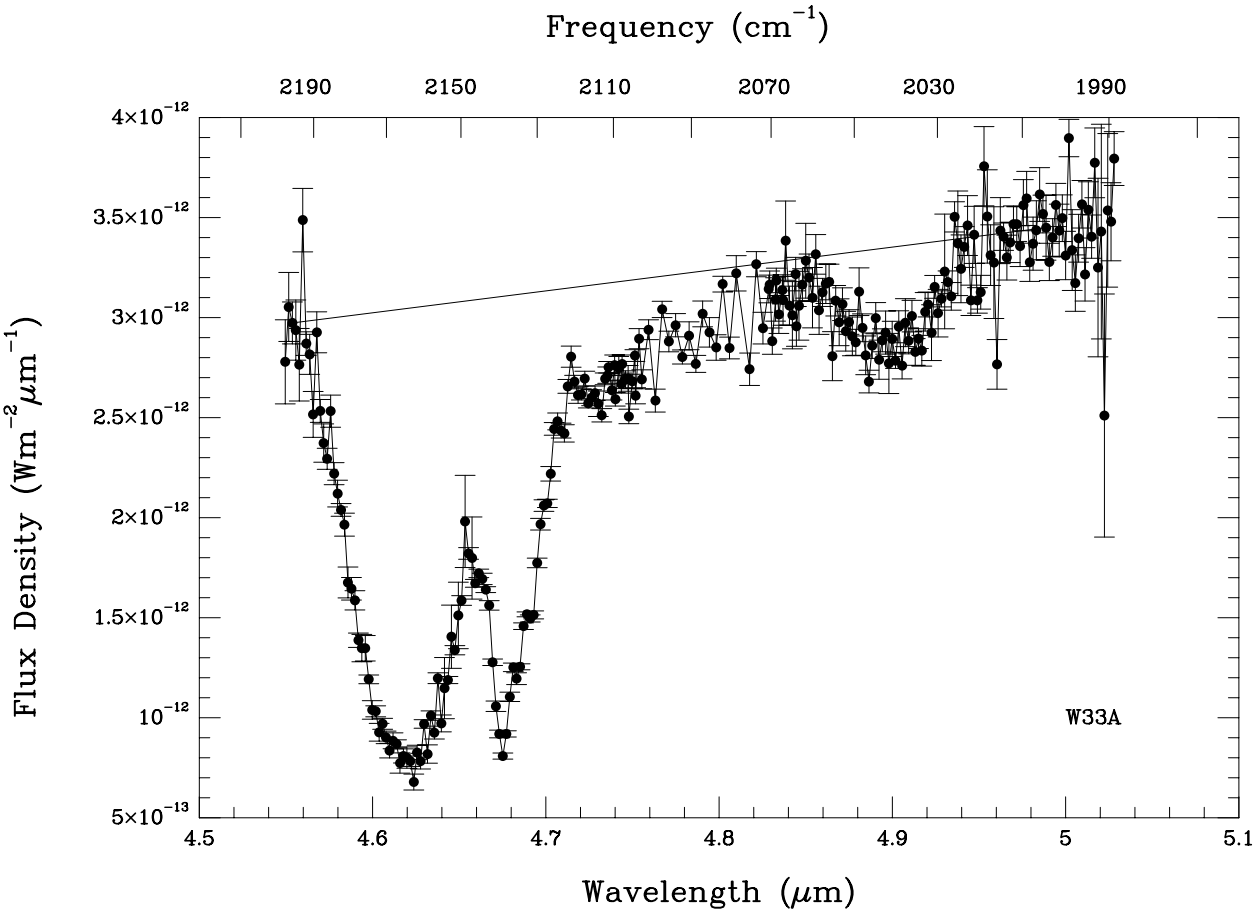

FIG. 1.—Flux spectra (W m^{-2} μm^{-1}) of W33 A 4.5–5.1 μm (2222–1960 cm^{-1}). The solid line depicts the continuum baseline from which the optical depth determinations were made.

TABLE 2

OPTICAL DEPTH OF ABSORPTION BANDS

Source	$\tau_{3.1}$ (H_2O)	$\tau_{3.47}$	$\tau_{3.5}$ Wing	$\tau_{4.62}$	$\tau_{6.8}$	$\tau_{4.67(CO)}$ Nonpolar 2140 cm^{-1}	$\tau_{4.67(CO)}$ Polar 2136 cm^{-1}	$\tau_{4.9}$ (OCS)	$\tau_{9.7}$ (Silicate)	Object A_V	$N(H)$ [a,b] (cm^{-2})
AFGL 2136	2.72[c]	...	...	0.06	...	0[b]	0.22[b]	...	5.07[c]	94.3[d]	1.8×10^{23}
AFGL 961 E	2.46[e]	0.68[f]	0.36[e]	0.06	...	0.22[g]	0.20[g]	<0.02	2.11[d]	39[b]	7.4×10^{22}
W33 A.....	5.4[d]	0.15[h]	2.53[d]	1.5	1.8[i]	0.79[g]	0.68[g]	0.14[j]	7.84[d]	145[k]	28×10^{22}
Elias 18.....	0.80[l]	0.022[f]	...	0.05[m]	...	0.26[g]	0.14[g]	...	0.43[l]	17–20[k]	2.2×10^{17}
Mon R2 IRS 2	2.54[e]	0.046[f]	0.46[e]	0.029	...	0.37[g]	0.16[g]	0.015[n]	2.11[b]	21[b]	4×10^{22}
L1551 IRS 5	2.1[o]	...	...	0.16[m]	...	0.80[m]	0.16[m]	...	1.4[b]	12.1[p]	2.3×10^{22}
Elias 16.....	1.6[m]	<0.031[q]	<0.016[e]	<0.05[m]	...	1.22[r]	0.11[g]	<0.04	0.66[l]	22.3[k]	3.8×10^{20}
NGC 7538 IRS 9.....	3.28[d]	0.10[f]	0.64[d]	0.31	0.3[r]	2.50[g]	0.2[g]	...	4.46[d]	84[s]	16×10^{22}

[a] From $N(H)/A_V = 1.9 \times 10^{21}$.
[b] Tielens et al. 1991.
[c] Hough et al. 1989.
[d] Willner et al. 1982.
[e] Smith, Sellgren, & Tokunaga 1989.
[f] Brooke, Sellgren, & Smith 1996.
[g] Chiar et al. 1998.
[h] Allamandola et al. 1992.
[i] Tielens & Allamandola 1987.
[j] Palumbo, Tielens, & Tokunaga 1995.
[k] Averaged from Elias 1978 and Smith, Sellgren, &, Brooke 1993.
[l] Whittet et al. 1988.
[m] Tegler et al. 1995.
[n] Palumbo et al. 1998.
[o] Sato et al. 1990.
[p] Elias 1978.
[q] Chiar, Adamson, & Whittet 1996.
[r] Schutte et al. 1996.
[s] Visual extinction in units of magnitudes from $\tau_{si} = A_V/18.6$.

TABLE 3

OPTICAL DEPTH RATIOS

Source	$\tau_{4.67(CO)}$ Nonpolar/Polar	$\tau_{4.62}/\tau_{4.67(CO)}$ Nonpolar	$\tau_{4.62}/\tau_{4.67(CO)}$ Polar	$\tau_{4.62}/A_V$	$\tau_{4.62}/\tau_{3.1}$	$\tau_{4.62}/\tau_{9.75}$	$\tau_{9.7}/\tau_{3.1}$
AFGL 2136	0	0	0.27	0.001	0.022	0.012	1.86
AFGL 961 E	1.1	0.27	0.30	0.002	0.024	0.028	0.86
W33A.....	1.2	1.9	2.21	0.01	0.278	0.191	1.45
Elias 18.....	1.9	0.19	0.36	0.003	0.063	0.116	0.54
Mon R2 IRS 2	2.3	0.078	0.18	0.001	0.011	0.014	0.83
L1551 IRS 5	5.0	0.20	1.0	0.013	0.076	0.114	0.67
Elias 16.....	11.1	0.041	0.45	0.002	0.031	0.076	0.41
NGC 7538 IRS 9.....	12.5	0.124	1.55	0.004	0.095	0.070	1.36

cm^{-1}) spectra of AFGL 961, AFGL 2136, AFGL 2591, Mon R2 IRS 2, and NGC 7538 IRS 9 are shown in Figures 2 and 3. The spectra show features at 4.62 μm (2165 cm^{-1}) and 4.67 μm (2140 cm^{-1}). In the case of W33 A, the broader spectral coverage reveals another absorption feature at 4.9 μm (2041 cm^{-1}). The 4.67 μm and 4.9 μm features are attributed to absorption by solid-phase carbon monoxide and carbonyl sulfide, and these are discussed elsewhere (Tielens et al. 1991 and Palumbo, Tielens, & Tokunaga 1995, respectively). A recent discussion of CO in these sources can be found in Chiar et al. (1998).

For the 4.62 μm and 4.67 μm features, a straight-line continuum was constructed between the data points near 4.56 and 4.76 μm (2190 and 2100 cm^{-1}). In the case of W33 A, where the observational coverage extended to 5.1 μm, the continuum was drawn from 4.55 to 4.98 μm (2197–2008 cm^{-1}). The optical depths derived from the W33 A spectra are shown in Figure 4, and optical depth plots for AFGL 961, AFGL 2136, NGC 7538 IRS 9, and Mon R2 IRS 2 are presented in Figures 5 and 6. Peak optical depths are listed in Table 2.

The profiles of the 4.62 μm band in W33 A and AFGL 961 are compared in Figure 7*a*. These are the only two sources with a strong enough 4.62 μm feature for such a comparison to be meaningful. Due to the strong solid CO band, there is an insufficient continuum to apply a χ^2 Gaussian fitting routine to these profiles. However, the peak positions in these sources agree to within 2.5 cm^{-1}, and the width of the feature agrees to within 5 cm^{-1}.

Gas-phase CO lines are known to be present in the spectra of many embedded objects (see Tielens et al. 1991 for discussion). Figure 3*a* shows the spectrum of the source AFGL 2591, in which the gas-phase CO lines are readily identified. A comparison to the spectra of Mon R2 IRS 2 and NGC 7538 IRS 9 (Fig. 3*b* and 3*c*, respectively), demonstrates the presence of weak CO lines in these sources as well. At low spectral resolution, blending of the rovibrational lines can give rise to broad absorption features that may

TABLE 4

SUMMARY OF CANDIDATE SPECIES

Candidate Molecule	Comments	Feasibility
Nitriles ($-C\equiv N$):		
Dicyandiamide [$NHC(NH_2)NHCN$]	Band at 2165 cm^{-1} but stronger 2204 cm^{-1} band is not observed.	Poor
Acetonitrile (methylcyanide) CH_3CN.....	Band at 2264 cm^{-1} in an H_2O matrix.	Poor
Pyruvonitrile (CH_3COCN)	Band at 2092 cm^{-1} in H_2O and 2225 cm^{-1} in argon.	Poor
Cyanogen (C_2N_2)	Band absorbs at 2167 cm^{-1} in solid state, but lab spectra show a band at 240 cm^{-1} 2 orders of magnitude stronger than 2165 cm^{-1}; not seen in ISM.	Poor
Thiocyanates ($S-C\equiv N$).....	No studies available.	Unknown
Isonitriles ($-N\equiv C$):	Typically stronger than nitriles, but less stable; might also expect the corresponding nitrile to be present.	
Methylisocyanide (isoacetonitrile) (CH_3NC).....	Absorbs at 2161 cm^{-1} in both gas phase and argon matrix; might expect related CH_3CN band at 2264 cm^{-1}; not seen in ISM.	Weak
N-butylisocyanide [$CH_3(CH_2)_3NC$]	Strong CN stretch near 2165 cm^{-1} in H_2O and argon matrices.	Weak
Methylisocyanoacetate (CH_3OCOCH_2NC)	Strong CN stretch near 2165 cm^{-1} in H_2O and argon matrices.	Weak
Isothiocyanates ($S-N\equiv C$)	No studies of isothiocyanates available.	Unknown
Cumulative double bonds ($C=C=O$):		
Ketene H_2C_2O.....	Absorbs at 2142 cm^{-1} in argon or O_2 ; need to see behavior in a more appropriate matrix.	Unknown
Cyanate ions (OCN^-)	Band falls in 2165–2222 cm^{-1} region; position sensitive to specific cation and solvation effects.	Good
Silanes:	Si—H stretch falls in the 2160–2140 cm^{-1} range.	
Organic silane ($-SiH_3$).....	Position varies with molecular group; possible that one can be found to match ISM feature.	Weak
Silane (SiH_4)	Bands at 2216, 2176 cm^{-1} in argon and 2200, 2165 cm^{-1} in H_2O; only one band detected in the ISM.	Poor

TABLE 5

PRODUCTION PATHWAYS

Starting Molecule	Product	Comments	References
		UV Photolysis of Ices	
CO, NH_3H_2O, CH_3OH ices	OCN^-	Presence of ions supported by experiments using electron donors/acceptors; C,N,O are implicated in the carrier	1, 2, 3, 4, 5, 6, 7, 8, 9, 10
N_2 mixtures	No 2165 cm^{-1} band		11
		Grain Surface Reactions	
Hydrogenation/nitrogen addition:			
H + CO	HCO		12
N + HCO	NCHO* to HNCO	Stabilization of the excited NCHO* to its lowest energy level, HNCO	13, 14
Acid-base chemistry:			
H_2O, NH_3, HNCO	OCN^-	Without UV. Deposition onto 12 K substrate yields OCN^- and NH_4^+, band at 2171 cm^{-1} grows during warm-up.	15
		Ion Bombardment of Ices	
$H_2O:CH_4:NH_3$ or N_2 ices (2:1:1)	R−O−CN	30–60 keV helium, argon ions; produces 2165 cm^{-1} band. R is a species belonging to the refractory residue	16
$H_2O:NH_3:CH_4$		($\simeq$1:3:2); MeV protons; produces 2170 cm^{-1} band	17
$H_2O:N_2:CO_2$		($\simeq$5:1:1 and 1:1:1); band at 2180 cm^{-1}	17

REFERENCES.—(1) Hagen 1982; (2) d'Hendecourt et al. 1986; (3) Allamandola et al. 1988; (4) Sandford & Allamandola 1990; (5) Bernstein et al. 1997; (6) Grim 1988; (7) Demyk et al. 1999; (8) Grim & Greenberg 1987b, (9) Grim et al. 1989a; (10) Schutte & Greenberg 1997; (11) Elsila et al. 1997; (12) van IJzendoorn et al. 1983; (13) Jacox & Milligan 1964; (14) Bernstein 1998; (15) Keane & Schutte 1998; (16) Palumbo et al. 1998; (17) Moore et al. 1983.

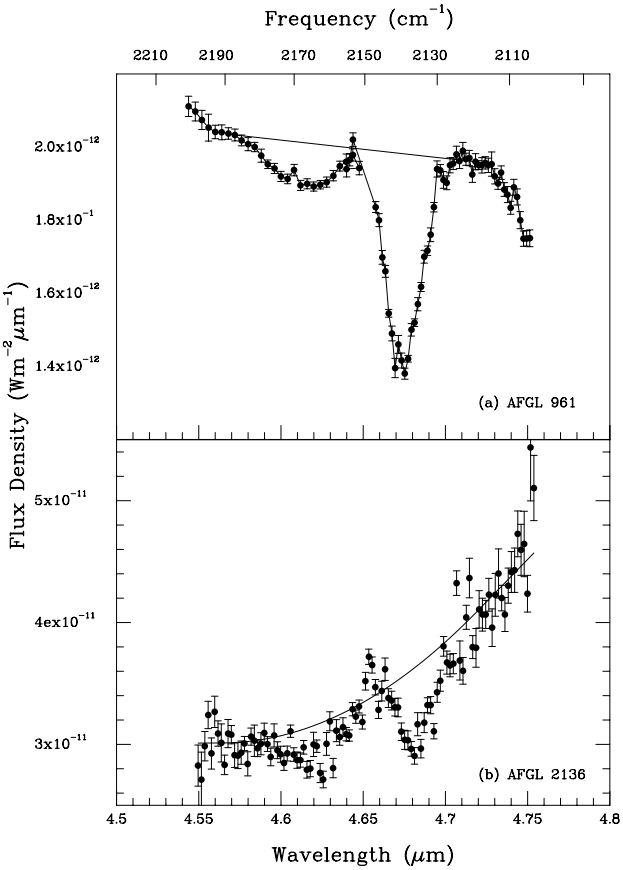

FIG. 2.—Flux spectra (W m^{-2} μm^{-1}) of (*a*) AFGL 961 and (*b*) AFGL 2136 from 4.5–4.8 μm (2222–2083 cm^{-1}). The solid line depicts the continuum baseline from which the optical depth determinations were made.

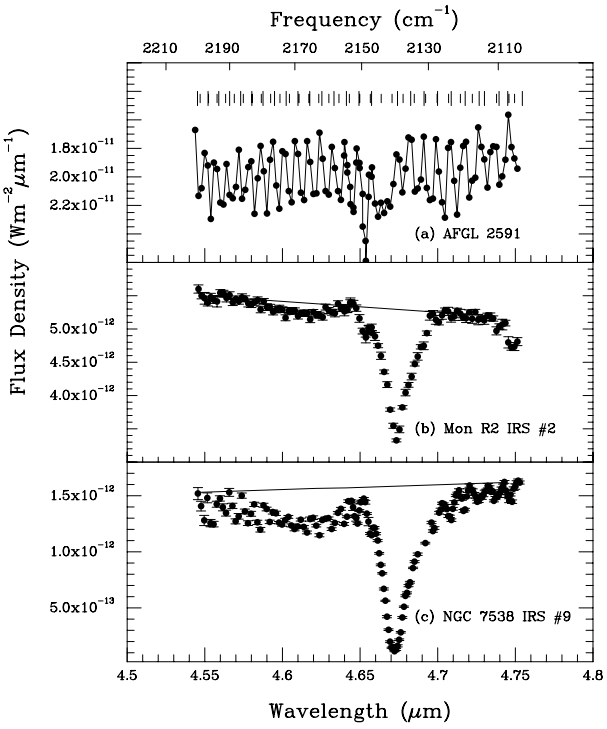

FIG. 3.—Flux spectra (W m^{-2} μm^{-1}) of (*a*) AFGL 2591, (*b*) Mon R2 IRS 2, and (*c*) NGC 7538 IRS 9 from 4.5–4.8 μm (2222–2083 cm^{-1}). Gas-phase CO lines (^{12}CO and ^{13}CO) have previously been identified in AFGL 2591 (Geballe & Wade 1985; Tielens et al. 1991) and are shown here for comparison to NGC 7538 IRS 9 and Mon R2 IRS 2 to illustrate the presence of CO gas-phase lines in the spectra of those sources. The solid line depicts the continuum baseline from which the optical depth determinations were made.

mimic solid-state absorptions (see Geballe 1986). However, at our resolution, the individual rovibrational lines are separated by more than one resolution element (see Fig. 3*a*), and blending will only occur for unreasonably large broadening parameters, i.e., $\delta v > 500$ km s^{-1}. Indeed, this is well in excess (by factors $\simeq 100$) of the width of CO individual rovibrational lines measured toward W33 A, NGC 7538 IRS 9, AFGL 2136, and AFGL 961 E (Mitchell et al. 1990). Moreover, there is no sign in our spectra of a corresponding *P*-branch of CO on the longer wavelength side of the 4.62 μm band, which should be equally strong compared to the *R*-branch if the 4.62 μm band were a result of gas-phase CO.

3.2. *Interrelationships of Absorption Features*

As shown in Table 2, the strength of the 4.62 μm band per unit A_V (total visual extinction) varies by about an order of magnitude from cloud to cloud. Apparent from Table 3 is the fact that the optical depth of the 4.62 μm band does not correlate with any other feature. The sources in Tables 2 and 3 are ordered from top to bottom in terms of decreasing temperature, as deduced from the amount of the volatile CO component (i.e., a nonpolar matrix) present relative to the amount of polar CO. The lack of correlation of the 4.62 μm band to the ice features may be indicative of (1) the location of the carrier of this material (i.e., circumstellar rather than intracloud dust), (2) the degree of processing to which the dust has been exposed, and/or (3) differences in the evolutionary stages of the embedded sources. It should be noted that none of the other features appear to correlate with each other either, which may simply be a reflection of the fact that the formation of these features is much more critically dependent upon the environmental conditions than was previously thought.

4. POSSIBLE IDENTIFICATIONS OF THE 4.62 MICRON BAND

The 4.62 μm band (Soifer et al. 1979; Lacy et al. 1984; Tegler et al. 1993, 1995), is commonly referred to in the literature as the X−C≡N band. The association of the interstellar feature with nitriles (−C≡N) came from early identifications with laboratory spectra thought to contain nitrile or isonitrile (−N≡C) groups. Although X− commonly refers to a halogen in chemistry circles, the use of X− in the astronomical literature simply denotes some undetermined species; we adopt this nomenclature here as well. The interstellar band has also been attributed to the cyanate ion (OCN^-) by several laboratory groups (Grim & Greenberg 1987a; Grim et al. 1989b; Schutte & Greenberg 1997; Demyk et al. 1999). Other candidates have been suggested in the literature as well, and they are summarized in Table 4. In some cases the proposed species has a feature that does not coincide with the position of the interstellar band, but the species has not been tested in an astrophysically relevant matrix. Until those experiments have been conducted, the candidate cannot be assessed completely.

Triple bond compounds including nitriles (X−C≡N), isonitriles (X−N≡C), thiocyanates (X−S−C≡N), iso-

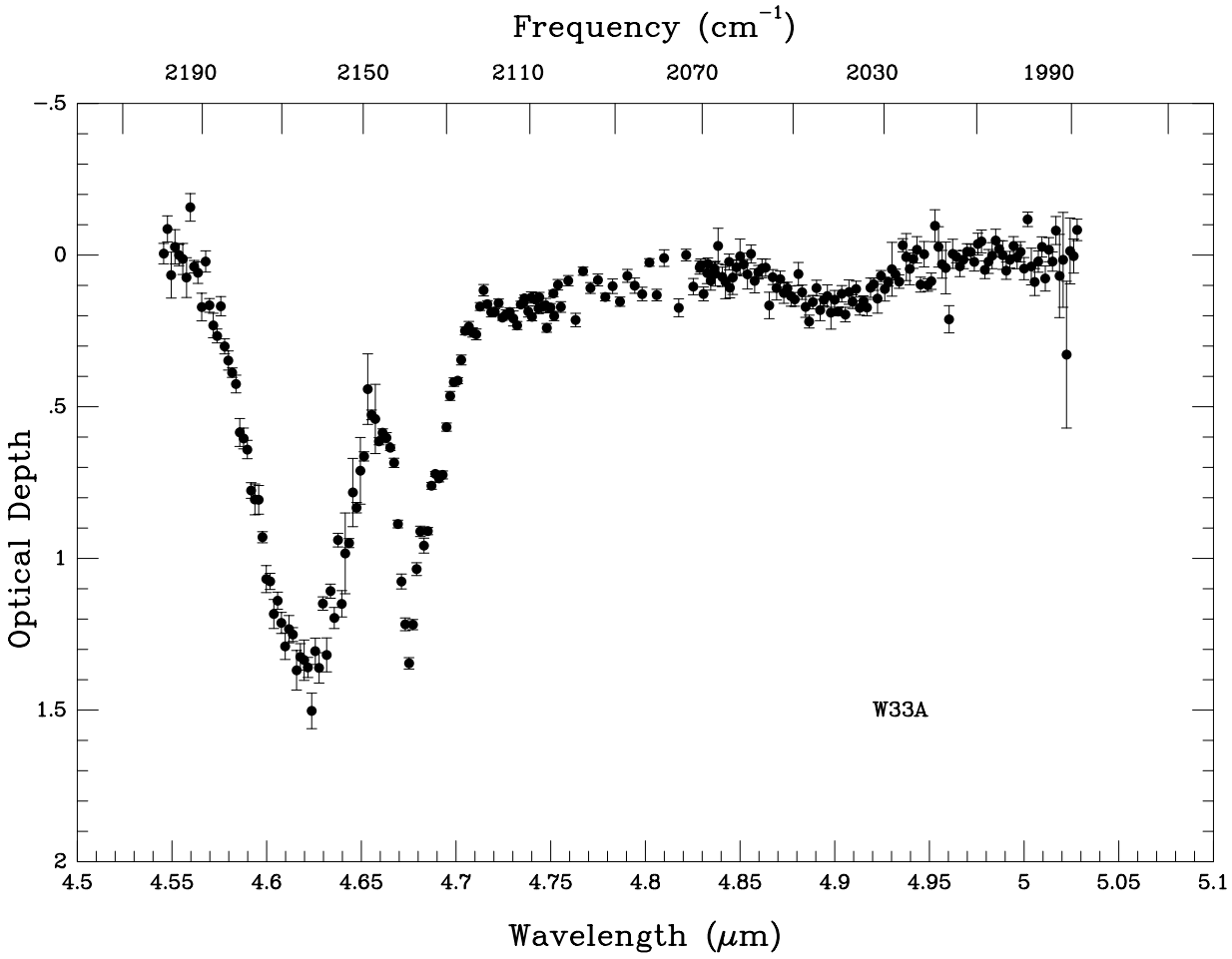

FIG. 4.—Optical depth plot from 4.5–5.1 μm (2222–1960 cm^{-1}) for W33 A

thiocyanates (X−N≡C−S), and cyanate ions (X−O−C≡N) are among those that appear in the 4–5 μm (2500–2000 cm^{-1}) region. Cumulative double bond species are also active in this region, and these include isocyanate ions (X−N=C=O) and ketenes (C=C=O). Cyanate ions will be discussed separately from the other candidates in the following section, as there has been substantially more laboratory investigation of these particular candidates.

4.1. *Nitriles and Isonitriles*

Most nitriles absorb at much higher frequencies (2200–2280 cm^{-1}) than the interstellar 4.62 μm (2165 cm^{-1}) band and are therefore not good candidate carriers (d'Hendecourt et al. 1986). In these cases, the spectra are not very sensitive to the matrix environment, so that there is little expectation that the peak wavelength might be shifted to the interstellar frequency in a different ice "environment." Among the specific nitriles that can be ruled out as the identification of the interstellar 4.62 μm band are dicyandiamide [(NHC(NH$_2$)NHCN)] and cyanogen (C_2N_2), because they have longer wavelength features that are not present in the observational data. Pyruvonitrile (CH_3COCN) had been proposed (d'Hendecourt et al. 1986), but subsequent experiments make this assignment seem unlikely (Bernstein et al. 1997). Nitriles that form strong hydrogen bonds with H_2O are an exception, however, because a substantial shift in the peak absorption frequency is seen in these cases. In the X−C≡N configuration, the presence of a lone electron pair on X allows hydrogen to bond with that atom, adjacent to the nitrile, and because of electron sharing between the nitrile and the X group, the H bond affects the peak position of the nitrile band (Bernstein et al. 1997).

Isonitriles absorb in the 2150–2175 cm^{-1} spectral range and, as such, are good candidates for the carrier of the interstellar 2165 cm^{-1} band (d'Hendecourt et al. 1986; Larson et al. 1985). Methyl isocyanide (CH_3NC; Larson et al. 1985) is such a candidate, because both in the gas phase and in an argon matrix CH_3NC absorbs at 2161 cm^{-1} (Khlifi et al. 1996; Freedman & Nixon 1972). The isonitriles, *n*-butylisocyanide [$CH_3(CH_2)3NC$] and methylisocyanoacetate (CH_3OCOCH_2NC), have also been considered as carriers of the interstellar 2165 cm^{-1} band (Bernstein et al. 1997). Both have a strong CN stretch near the interstellar 2165 cm^{-1} band in argon and H_2O matrices (Bernstein et al. 1997). However, one general, indirect argument against all isocyanides is that their abundance might reasonably be expected to be less than that of the corresponding cyanide, and no bands in the general nitrile spectral region (where cyanides would appear) have been seen (Whittet et al. 1996). For this reason, the feasibility label for isonitriles in Table 4 is "weak."

4.2. *Species with Cumulative Double Bonds*

Among species with cumulative double bonds are ketenes (C=C=O). Ketenes absorb in the range 2080–2200 cm^{-1},

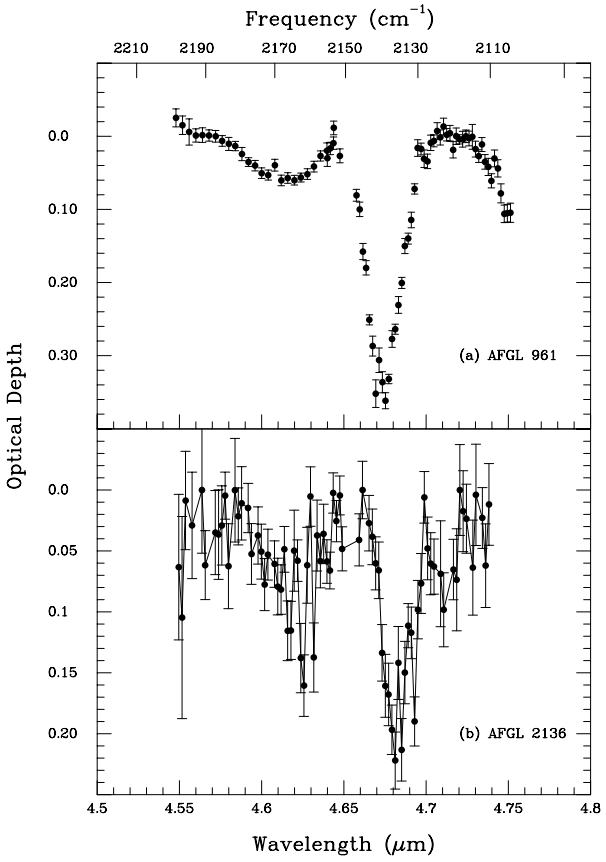

FIG. 5.—Optical depth plot from 4.5–4.8 μm (2222–2083 cm^{-1}) for (*a*) AFGL 961 and (*b*) AFGL 2136.

often near 4.65 μm (2150 cm^{-1}) (Socrates 1980). In an argon or O_2 matrix, the compound ketene (H_2C_2O) absorbs at 4.67 μm (2142 cm^{-1}) (Moore & Pimentel 1963), which is close enough to the interstellar position to speculate that in

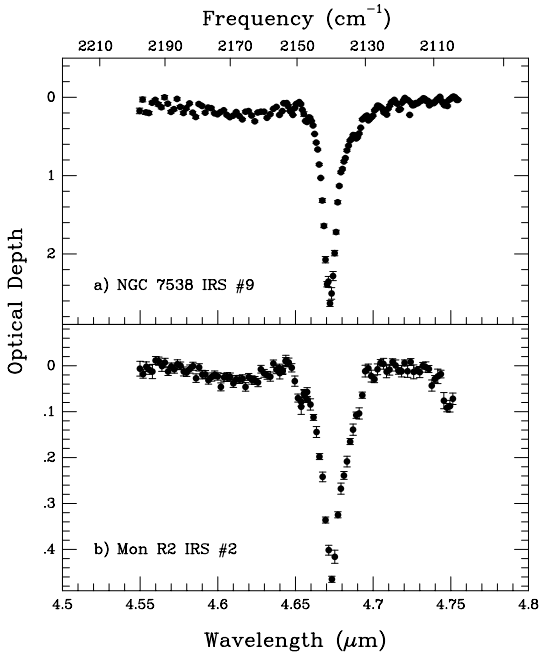

FIG. 6.—Optical depth plot from 4.5–4.8 μm (2222–2083 cm^{-1}) for (*a*) NGC 7538 IRS 9 and (*b*) Mon R2 IRS 2.

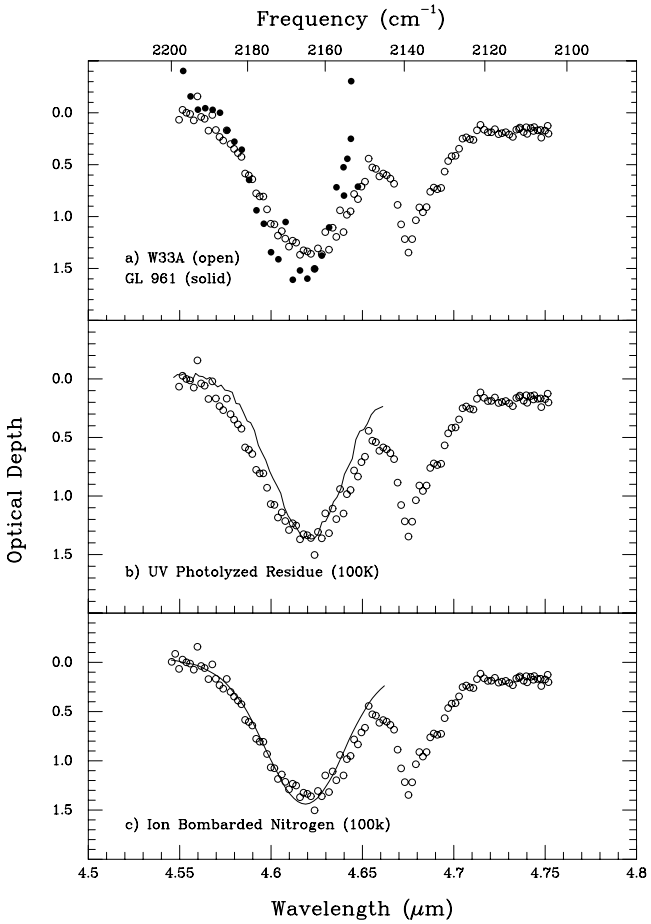

FIG. 7.—The 4.5–4.8 μm (2222–2083 cm^{-1}) flux spectra of (*a*) AFGL 961 (*filled circles*) scaled to W33 A (*open circles*); for clarity, only the points relevant to the 4.62 μm band are shown for W33 A. (*b*) The UV photolyzed residue produced when an H_2O:CH_3OH:CO:NH_3 = 100:50:10:10 ice is irradiated at 12 K and subsequently warmed to 100 K (taken from Bernstein et al. 1995; *solid line*) compared to the observational data from W33 A (*open circles*). (*c*) The organic residue produced through 3 keV He^+ ion bombardment of a mixture containing H_2O:N_2:CH_4 = 1:1:1 compared to the observational data for W33 A (*open circles*). The dose received by the mixture was 40 eV per 16 amu, and the spectrum shown is after warm-up to 100 K (Palumbo et al. 1998) (*solid line*).

an H_2O matrix ketene might be a viable candidate. Laboratory experiments to investigate the peak position of ketene absorption in astrophysically relevant matrices (such as H_2O, CO, and CO_2) are needed.

4.3. *The Cyanate Ion*

The strong CN stretching vibration in simple cyanate salts falls in the range 4.5–4.62 μm (2225–2165 cm^{-1}). For example, NH_4NCO absorbs at 2217 cm^{-1} (Hubbard et al. 1975) Grim & Greenberg (1987a); Schutte & Greenberg (1997); Demyk et al. (1999) have identified the 4.62 μm band in their laboratory spectra, generated by FUV photolysis, as the cyanate (OCN^-) ion and suggest that this ion is the carrier of the interstellar band. The laboratory spectra compare favorably with the interstellar 4.62 μm band (Fig. 7*b*), and for this reason we have assigned its feasibility as "good" in Table 4.

4.4. *Thiocyanates*

The C≡N stretching vibrations in thiocyanates (S−TC≡N) is observed in the range 2140–2175 cm^{-1}

(Socrates 1980). There have been no studies made thus far to test their relevance to the interstellar 4.62 μm (2165 cm^{-1}) band.

4.5. *Silanes*

Organic silane ($-SiH_3$) compounds have also been considered candidates for the interstellar 4.62 μm (2165 cm^{-1}) band (Nuth & Moore 1988; Moore, Tanabe, & Nuth 1991). The Si–H stretch in organic silanes ($-SiH_3$) falls in the range 2160–2140 cm^{-1} (Socrates 1980). Silane (SiH_4) has two absorption bands, at 2216 and 2176 cm^{-1} (in argon) and 2200 and 2165 cm^{-1} (in H_2O) (Lloret & Abouaf-Marguin 1986; Nuth & Moore 1988). Only one band is detected in the interstellar spectra, and therefore SiH_4 itself is not a good candidate. In addition, we note that hydrogen bonded to silicon surfaces shows Si–H stretching modes in the range 2200–2000 cm^{-1}; the exact position will depend on the molecular group attached. For silicate surfaces, the oxidized monohydride [Si_3O_3Si-H] absorbs at 2250 cm^{-1}. For silicon surfaces, the monohydride [Si_3Si-H] absorbs at 2082 cm^{-1}, and the dihydride [Si_2SiH_2] absorbs at 2133 cm^{-1} (Watanabe & Sugati 1996). Presumably there is a silicon hydride that falls near 2165 cm^{-1}, but until laboratory spectra reveal such a band, the feasibility of silanes must be labeled "weak" in Table 4.

4.6. *Summary of Candidate Species*

In the literature, a number of likely candidates have been proposed for the interstellar 4.62 μm (2165 cm^{-1}) band (see Table 4). A few of the specific proposed carriers can be confidently eliminated (dicyandiamide, cyanogen, and SiH_4) because the stronger, corresponding infrared absorption bands of these species have not been observed. Others, such as acetonitrile and pyruvonitrile, are rejected because they absorb at the wrong wavelengths. A number of other general types of compounds are candidates (i.e., isonitriles and organic silanes), but a likely specific molecule has not been put forward and further study is required. Additional candidates that require laboratory study include thiocyanates, isothiocyanates, and ketenes. The cyanate ion may be the most promising candidate of all. It is always difficult to identify with confidence a compound from one spectral feature, and hence a true identification of the carrier of the 4.62 μm band still cannot be made on spectroscopic arguments alone. Other features have been searched for, but within the limited data available (Tables 2 and 3) no other absorption feature correlates with the interstellar 4.62 μm band. As the data reduction techniques for evaluation of the data from *ISO* improve, it is likely that weaker features will be probed more effectively, and bands related to the 2165 cm^{-1} carrier may be identified. This will greatly assist in the assessment of the possible carriers presently under consideration.

5. PRODUCTION PATHWAYS TO THE INTERSTELLAR 4.62 MICRON BAND

The pathway toward production of the interstellar 4.62 μm band is a complex issue. From the laboratory data currently available, 4.62 μm bands similar in profile can be produced from ice mixtures containing nitrogen, carbon, and oxygen, which are exposed to either ultraviolet photolysis or ion bombardment. Accepting, for the moment, the identification of the interstellar 4.62 μm band with the 4.62 μm band produced by processing ice analogs, we will now discuss the possible pathways toward the interstellar feature. Energetic processing of interstellar ices, either through ultraviolet photolysis, ion bombardment, or both, and grain surface chemistry are all plausible pathways by which the interstellar 4.62 μm band might arise. Only ion bombardment, however, has been shown to form the 4.62 μm band if the nitrogen is in the form of solid N_2. The discovery that solid N_2 comprises the majority of the ice present on bodies in the outer solar system (Cruikshank et al. 1993, 1998) suggests that the infrared inactive N_2 may be hiding in the interstellar ices as well (Ehrenfreund et al. 1997; Elsila, Allamandola, & Sandford 1997). Therefore, studies of the interstellar 4.62 μm (2165 cm^{-1}) band may provide information on both the reservoir of the solid-state nitrogen in interstellar ices and the energetic process by which it participates in the chemistry of the carrier of the 4.62 μm band. Identifying the production mechanism is therefore directly related to identifications of the interstellar ice constituents that reside on the preprocessed grain mantle. Here we discuss each of these in turn, and they are summarized in Table 5.

5.1. *FUV Laboratory Studies*

The role of ultraviolet photolysis is one of the key questions in the chemistry of interstellar ices. Theoretical and experimental studies have long suggested that FUV photolysis of interstellar ices is important for their composition and the X–CN band is often cited in support of this hypothesis (Greenberg & Yencha 1973; d'Hendecourt et al. 1986; Allamandola, Sandford, & Valero 1988; Grim et al. 1989a; Grim & Greenberg 1987; Schutte et al. 1996; Bernstein et al. 1996). Laboratory far-ultraviolet (FUV) photolysis of ices containing CO and NH_3 show a prominent absorption feature at 4.62 μm (2165 cm^{-1}) (Hagen 1982; Lacy et al. 1984; d'Hendecourt et al. 1986; Grim 1988; Grim & Greenberg 1987a; Allamandola et al. 1988; Schutte & Greenberg 1997). Figure 7*b* illustrates the good comparison between the FUV photolysis laboratory and interstellar data.

While the first experiments were interpreted in terms of an otherwise unidentified nitrile, very soon afterward the ion OCN^- was implicated (Grim & Greenberg 1987a; Grim et al. 1989a; Schutte & Greenberg 1997). Recent laboratory studies using electron donors and acceptors support this ion identification for the laboratory-produced 4.62 μm band (Demyk et al. 1999). The ion is thought to result from an acid-base reaction between NH_3 and FUV-produced HNCO (Grim et al. 1989a; Schutte & Greenberg 1997).

One problem for any ion identification is the charge balance. For each negative ion made, a positive ion must be produced. In these experiments, the proposed counter-ion is NH_4^+, and a band in the range 6.6–6.9 μm (1450–1500 cm^{-1}), depending on the matrix, is attributed to this ion (Grim & Greenberg 1987a; Demyk et al. 1999). There is a strong band in interstellar ice spectra at about 6.8 μm, but whether the NH_4^+ band falls at this position in astrophysically relevant matrices is not clear yet. Nor has the charge balance in interstellar ices been completely evaluated. The sensitivity of the strength and peak position of the NH_4^+ band to the molecular environment in the laboratory studies (Demyk et al. 1999) might indicate that such an analysis will be difficult.

5.2. *Ion Bombardment of Ices*

An alternative way to process interstellar ice mixtures is through bombardment with high-energy protons. Moore et al. (1983) have shown that a band is produced at 2170 cm^{-1} upon the irradiation of a mixture of H_2O:NH_3:CH_4 ($\simeq$1:3:2) after irradiation with $\simeq$MeV protons. They also found that irradiation of mixtures H_2O:N_2:CO_2 ($\simeq$1:1:1) and H_2O:N_2:CO ($\simeq$5:1:1) produces a band at about 2180 cm^{-1}. It is well established (e.g., Strazzulla & Johnson 1991; Strazzulla 1997, 1998) that ion irradiation drives the formation not only of specific molecules, depending on the particular target, but also of refractory residues. Especially promising is recent work (e.g., Palumbo et al. 1998) that includes N_2 in the starting mixture and produces a band that is quite similar to the interstellar band. Ion bombardment, which is analogous to cosmic-ray interactions with icy dust grains in dense molecular clouds, has the advantage that the high-energy ions can break N_2. The resulting 4.62 μm band is discussed in Palumbo et al. (1998) and compares well to the interstellar data for W33 A (Fig. 7*c*). It is unclear whether the 4.62 μm band produced by ion bombardment is also due to the OCN^- ion.

Laboratory studies have shown that UV photolysis of N_2-containing mixtures cannot produce a 4.62 μm band (Elsila et al. 1997), because the energy from the UV lamps is insufficient to break apart the N_2. While the interstellar radiation field contains photons more energetic (i.e., in the range 912–1250 Å) than these laboratory lamps, FUV photolysis at best will be very inefficient.

5.3. *Grain Surface Reactions*

It is also possible that the carrier of the 4.62 μm band is produced via simple grain surface chemistry, followed by the acid-base reactions outlined in § 5.1 (Keane & Schutte 1999). Laboratory studies have shown that even in the absence of FUV irradiation codeposited HNCO and NH_3, in various astrophysical relevant ice mixtures, undergoes an acid-base reaction forming OCN^- and NH_4^+ (Keane 1997; Keane & Schutte 1999). While not all of the HNCO is converted in these experiments, upon warm-up to 80 K much of the remaining HNCO undergoes the acid–base reaction, and the spectrum is dominated by the 4.62 μm band. HNCO and NH_3 might both result from grain surface chemistry. Ammonia can be formed through hydrogenation of accreted atomic N. HNCO might result from chemistry initiated by the reaction of H + CO forming HCO (van IJzendoorn et al. 1983). This radical can react with N and the intermediate excited complex NCHO* might relax to the energetically most favorable isomer HNCO (Charnley 1997; 1999). Alternatively, this route might actually lead to NH_2CHO (Tielens & Hagen 1982), a species that has been observed in the gas phase in the ISM (Kuan & Snyder 1996), but which has no solid-state 4.62 μm band. Further studies of this grain surface route are needed.

6. CONCLUSIONS

We present new infrared spectra of dust embedded protostars that reveal a strong absorption feature near 4.67 μm (2141 cm^{-1}) and a weaker absorption feature centered near 4.62 μm (2165 cm^{-1}). The feature near 4.67 μm (2141 cm^{-1}) has previously been identified as absorption due to solid CO within the icy grain mantle (Tielens et al. 1991). The 4.62 μm (2165 cm^{-1}) band, however, has not yet been unambiguously identified. The band present throughout our sample of five embedded protostars was previously reported in a small number of other protostellar objects (Lacy et al. 1984; Tegler et al. 1993; Tegler et al. 1995; Weintraub et al. 1994), demonstrating that the feature probably forms fairly readily in protostellar regions. The interstellar 4.62 μm (2165 cm^{-1}) band does not vary more than 2.5 cm^{-1} in position, suggesting the carrier of the band may be fairly insensitive to changes in the local environment. Gas-phase CO absorption is detected in the spectra of some of these sources, but blending of gas-phase CO is not responsible for the broad, shallow absorption at 4.62 μm (2165 cm^{-1}). The 4.62 μm (2165 cm^{-1}) band does not correlate with any other absorption feature in the spectra of these sources; however, there is in general a lack of correlation among the ice absorption features in these sources. The 4.62 μm band may therefore simply be a part of that same trend, perhaps indicating the carriers of these features are sensitive to environmental conditions in the cloud.

Our study samples protostars from different molecular clouds and shows that the strength of the 4.62 μm band per unit A_V (total visual extinction) varies by about an order of magnitude from cloud to cloud. Such a disparity may indicate that different processes (i.e., UV photolysis, ion bombardment, grain surface chemistry, or thermal processes) are involved in the production of the 4.62 μm band or, more likely, that differing evolutionary states of the embedded objects obfuscate the situation. It is noteworthy that in every case in which the 4.62 μm feature was searched for, an absorption band was found.

We have investigated a variety of possible identifications for the interstellar 4.62 μm band. Good fits to the interstellar spectra are obtained with the OCN^- ion produced either by acid-base reactions (Keane & Schutte 1999) or through FUV photolysis of NH_3-containing ices (Schutte & Greenberg 1997; Demyk et al. 1999), as well as with an organic residue produced through ion bombardment of nitrogen-containing ices (Moore et al. 1983; Palumbo et al. 1998). A number of other species may be feasible candidates as well, but relevant laboratory data are incomplete.

We have reviewed proposed formation mechanisms for the production of the 4.62 μm band, such as UV photolysis, ion bombardment, and/or grain surface chemistry assisted by acid-base reactions in interstellar ices. Organic residues produced by energetic processing of astrophysically plausible initial ice mixtures reproduce the 4.62 μm (2165 cm^{-1}) band in general peak position and profile quite well. Ion bombardment has the advantage that it would allow N_2, possibly the dominant nitrogen reservoir in molecular clouds, to participate in the chemistry of the ices. The issues to consider in trying to discriminate between these processes are the nitrogen budget in interstellar ices (i.e., NH_3 or N_2), the efficiency of FUV photolysis versus particle bombardment, and the detailed grain surface reaction schemes. None of these are well determined at this time.

This paper benefited from careful review of an anonymous referee and from conversations with several colleagues. Among these, we thank especially Steve Charnley, Jean Chiar, Cristina Dalle Ore, and Elisabetta Palumbo. We also thank Karin Demyk, Louis d'Hendecourt, Jacqueline Keane, Willem Schutte, Elisabetta Palumbo, and

Giovanni Strazzulla for sharing their data in advance of publication. We thank the telescope operators at the NASA IRTF and the support staff of Mauna Kea Observatory. This work was partially supported by NASA grants 185-52-12-09 (Y. J. P.), 188-44-21-04 (Y. J. P.), and 399-20-10-27(A. G. G. M. T.).

REFERENCES

Allamandola, L. J., Sandford, S. A., Tielens, A. G. G. M., & Herbst, T. M. 1992, ApJ, 399, 144
Allamandola, L. J., Sandford, S. A., & Valero, G. 1988, Icarus, 76, 225
Bernstein, M. P. 1998
Bernstein, M. P., Sandford, S. A., & Allamandola, L. J. 1996, ApJ, 472, 127
———. 1997, ApJ, 476, 932
Bernstein, M. P., Sandford, S. A., Allamandola, L. J., Chang, S., & Scharberg, M. A. 1995, ApJ, 454, 327
Brooke, Sellgren, & Smith 1996, ApJ, 459, 209
Charnley, S. B. 1997, in Astronomical and Biochemical Origins and the Search for Life in the Universe, ed. C. B. Cosmovici, S. Bowyer, & D. Wertheimer (Bologna: Editrice Compositori), 89
———. 1999, ApJ, submitted
Chiar, J. E., Adamson, A. J., & Whittet, D. C. B. 1996, ApJ, 472, 665
Chiar, J. E., Gerakines, P. A., Whittet, D. C. B., Pendleton, Y. J., Tielens, A. G. G. M., Adamson, A. J., & Boogert, A. C. A. 1998, ApJ, 498, 716
Cruikshank, D. P., et al. 1993, Science, 261, 742
———. 1998, in Solar System Ices, ed. B. Schmitt, M. Festou, & C. de Bergh (Dordrecht: Kluwer), 655
Demyk, K., Dartois, E., d'Hendecourt, L., Jourdain de Muizon, M., Heras, A. M., & Breitfellner, M. 1999, A&A, 339, 553
d'Hendecourt, L. B., et al. 1996, A&A, 315, 365
d'Hendecourt, L. B., Allamandola, L. J., Grim, R. J. A., & Greenberg, J. M. 1986, A&A, 158, 119
Ehrenfreund, P., Boogert, A. C. A., Gerakines, P. A., Tielens, A. G. G. M., & van Dishoeck, E. F. 1997, A&A, 328, 649
Elias, J. H. 1978, ApJ, 224, 857
Elsila, J., Allamandola, L. J., & Sandford, S. A. 1997, ApJ, 479, 818
Freedman, T. B., & Nixon, E. R. 1972, Spectrochim. Acta, 28A, 1375
Geballe, T. R. 1986, A&A, 162, 248
Geballe, T. R., & Wade, R. 1985, ApJ, 291, L55
Greenberg, J. M., & Yencha, A. J. 1973, in IAU Symp. 52, Interstellar Dust and Related Topics, ed. J. M. Greenberg & H. C. van de Hulst (Dordrecht: Reidel), 309
Grim, R. J. A. 1988, Ph.D. thesis, Rijks Univ., Leiden
Grim, R. J. A., & Greenberg, J. M. 1987a, ApJ, 321, L91
———. 1987b, A&A, 181, 155
Grim, R. J. A., et al. 1989a, A&AS, 78, 161
Grim, R. J. A., Greenberg, J. M., Schutte, W. A., & Schmitt, B. 1989b, ApJ, 341, L87
Hagen, W. 1982, Ph.D. thesis, Rijks Univ., Leiden
Hough, J. H., Whittet, D. C. B., Sato, S., Yamashita, T., Tamura, M., Nagata, T., Aitken, D. K., & Roche, P. F. 1989, MNRAS, 241, 71
Hubbard, J. F., Voeks, G. E., Hobby, G. L., Ferris, J. P., Williams, D. A., & Nicoderm, D. E. 1975, J. Mol. Evol., 5, 23
Jacox, M. E., & Milligan, D. E. 1984, J. Chem. Phys., 40, 2457
Keane, J. 1997, M.A. thesis, Rijks Univ., Leiden
Keane, J., & Schutte, W. A. 1999, A&A, submitted
Khilifi, M., Paillous, P., Bruston, P., Raulin, F., & Guillemin, J.-C. 1996, Icarus, 124, 318
Kuan, Y., & Snyder, L. 1996, ApJ, 470, 981
Lacy, J. H., Baas, F., Allamandola, L. J., Persson, S. E., McGregor, P. J., Lonsdale, C. J., Geballe, T. R., & van de Bult, C. E. P. M. 1984, ApJ, 276, 533
Larson, H. P., Davis, D. S., Black, J. H., & Fink, U. 1985, ApJ, 299, 873
Lloret, A., & Abouaf-Marguin, L. 1986, J. Chem. Phys., 107, 139
Mitchell, G. F., et al. 1990, ApJ, 554, 573
Moore, C. B., & Pimentel, G. C. 1963, J. Chem. Phys., 38, 2816
Moore, M. H., Bertram, D., Khanne, R., & A'Hearn, M. F. 1983, Icarus, 54, 388
Moore, M. H., Tanabe, T., & Nuth, J. A. 1991, ApJ, 373, L31
Nuth, J. A., & Moore, M. H. 1988, ApJ, 373, L113
Palumbo, M. E., Tielens, A. G. G. M., & Tokunaga, A. T. 1995, ApJ, 449, 674
Palumbo, M. E., Strazzulla, G., Pendleton, Y. J., & Tielens, A. G. G. M. 1998, A&A, submitted
Sandford, S. A., & Allamandola, L. J. 1990, ApJ, 355, 357
Sato, S., Nagata, T., Tanaka, M., & Yamamoto, T. 1990, ApJ, 359, 192
Schutte, W. A., & Greenberg, J. M. 1997, A&A, 317, L43
Schutte, W. A., Gerakines, P. A., Geballe, T. R., van Dishoeck, E. F., & Greenberg, J. M. 1996, A&A
Smith, R. G., Sellgren, K., & Brooke, T. Y. 1993, MNRAS, 263, 749
Smith, R. G., Sellgren, K., & Tokunaga, A. T. 1989, ApJ, 344, 413
Socrates, G. 1980, Infrared Characteristic Group Frequencies: Tables and Charts (New York: Wiley)
Soifer, B. T., Puetter, R. C., Russel, R. W., Willner, S. P., Harvey, P. M., & Gillet, F. C. 1979, ApJ, 232, L53
Strazzulla, G., & Johnson, R. E. 1991, in Comets in the Post-Halley Era, ed. R. L. Newburn, Jr., M. Neugebauer, & J. Rahe (Dordrecht: Kluwer), 1, 243
Strazzulla, G. 1997, in From Stardust to Planetesimals, ed. Y. J. Pendleton & A. G. G. M. Tielens (San Francisco: ASP), 122, 423
Strazzulla, G. 1998 in: Solar System Ices, ed. B. Schmitt, C. de Bergh, & M. Festou (Dordrecht: Kluwer), 281
Tegler, S. C., Weintraub, D. A., Allamandola, L. J., Sandford, S. A., Rettig, T. W., & Campins, H. 1993, ApJ, 411, 260
Tegler, S. C., Weintraub, D. A., Rettig, T. W., Pendleton, Y. J., Whittet, D. C. B., & Kulesa, C. A. 1995, ApJ, 439, 279
Tielens, A. G. G. M., & Allamandola, L. J. 1987, in Physical Processes in Interstellar Clouds, ed. G. E. Morfill & M. Scholer (Dordrecht: Reidel), 333
Tielens, A. G. G. M., & Hagen, W. 1982, A&A, 114, 245
Tielens, A. G. G. M., Tokunaga, A. T., Geballe, T. R., & Baas, F. 1991, ApJ, 381, 181
Tokunaga, A. T., Smith, R. G., & Irwin, I. 1987, in Infrared Astronomy with Arrays, ed. C. G. Wynn-Williams & E. E. Becklin (Honolulu: Univ. Hawaii), 367
van IJzendoorn, L., Allamandola, L. J., Baas, F., & Greenberg, J. M. 1983, J. Chem. Phys., 78, 7019
Watanabe, S., & Sugati, Y. 1996, Appl. Surface Sci., 107, 90
Weintraub, D. A., Tegler, S. C., Kastner, J. H., & Rettig, T. W. 1994, ApJ, 423, 674
Whittet, D. C. B., Bode, M. F., Longmore, A. J., Adamson, A. J., McFadzeon, A. D., Aitken, D. K., & Roche, P. F. 1988, MNRAS, 233, 321
Whittet, D. C. B., et al. 1996, A&A, 315, 357
Willner, S. P., et al. 1982, ApJ, 253, 174